Anal. Bioanal. Electrochem., Vol. 16, No. 5, 2024, 438-458
https://www.doi.org/10.22034/abec.2024.2027869.1448

Analytical & Bioanalytical Electrochemistry

Full Paper

Evaluation of Uniform and Localized Corrosion Behaviour of Aluminum Alloy 1050 as Al/AgO Battery Anode in 6.0 M KOH in the Presence of an Organosulfur Inhibitor

Hamed Pourfarzad,[1,2,*] and Mohammad Peirow Asfia[3]

[1]*Center of Excellence in Electrochemistry, University of Tehran, Tehran, Iran*
[2]*Department of Analytical Chemistry, University of Kashan, Kashan, P.O. Box 15875-4413, Iran*
[3]*Department of Materials and Metallurgical Engineering, Amirkabir University of Technology (Tehran Polytechnic), Hafez Ave., P.O. Box 15875–4413, Tehran, Iran*

*Corresponding Author, Tel.: +989100998568
E-Mail: h.pourfarzad2030@gmail.com

Received: 13 March 2024 / Received in revised form: 18 May 2024 / Accepted: 26 May 2024 / Published online: 31 May 2024

Abstract- The evaluation of the Aluminum alloy 1050 as an anode in an Al/AgO battery in an aerated 6.0 M KOH solution involves studying its corrosion behavior and battery performance. Various techniques, including potentiodynamic polarization, electrochemical impedance spectroscopy, electrochemical noise analysis, field-emission scanning electron microscopy, energy-dispersive X-ray spectroscopy, and galvanostatic discharge, are employed to assess these aspects. The polarization results reveal that the addition of various concentrations of thiourea to ZnO as the best-mixed inhibitor reduces the corrosion rate of aluminum during the initial stages from 4638.9 mpy to 1634.6 mpy. Also, this type of inhibitor leads to an increase in polarization resistance from 3.10 $\Omega.cm^2$ to 8.36 $\Omega.cm^2$, which are in good agreement with the results of impedance spectroscopy studies. Furthermore, based on the findings of EIS studies this type of inhibitor with an inhibition efficiency of more than 90.47%, facilitates the formation of a protective layer on the surface, effectively controlling the initiation and propagation of pits. As the immersion time increases, the inhibitor creates conditions where the aluminum anode corrodes uniformly, providing the necessary electrons and capacity for the battery to perform better. The SEM results also demonstrate that the corrosion of aluminum becomes more uniform, resulting in an impressive anode efficiency of 90.19% in the galvanostatic discharge test.

Keywords- Citrus sinensis; CuO nanoparticles; ZnO nanoparticles; CuO-ZnO nanocomposite; Electrochemical detection; Hydrogen peroxide

1. INTRODUCTION

Extensive research into advanced and nontoxic energy conversion and storage devices has been launched as a result of the growing demand for cleaner, safer, or more efficient energy sources [1-4]. Electrochemical systems like batteries, fuel cells, and supercapacitors are essential in the field for energy generation, transformation, and storage [2-9]. Within this field, electrochemical systems such as batteries, fuel cells, and supercapacitors play a crucial role in generating, transforming, and storing energy [2-9]. Compared to traditional nickel-cadmium and lead acid batteries, lithium batteries are particularly desirable because of their powerful electrical characteristics, large energy density, long service life as well as durability. The cathode and anode, however, are the limits of Li-ion battery energy density because their specific capacity is set by the weight of active materials, mainly metal oxides such as $LiCoO_2$ (130 $mAhg^{-1}$) for the cathode and graphite (170 $mAhg^{-1}$) for the anode, which function as bottlenecks. Consequently, Li-ion battery energy density is between 120 and 265 $wh.kg^{-1}$. Consequently, the electrode chemistry of conventional Li-ion batteries limits the practical energy density, which limits the advancements in lithium-ion battery technology [10,11].

Since then, silver oxide-based batteries, like Zinc-Silver oxide batteries (ZSOB), have been used extensively in many different industries because they offer the most energy per unit of weight and volume when compared to other aqueous secondary batteries. These batteries have an energy density value of up to 300 Wh kg^{-1}, which is higher than even the market leader lithium-ion batteries, which typically range from 120 to 200 $Wh.kg^{-1}$. Also, when it comes to the early phases of charge-discharge cycling, Zinc-Silver oxide batteries provide an amazing power density of about 600 W kg^{-1}, which is much higher than the best lithium-ion batteries that are currently available—less than 265 $W.kg^{-1}$. Finally, because of their water-based electrolytes, Zinc-Silver oxide batteries are thought to be inherently safe [12].

With the same volume and weight, an aluminum-silver oxide battery can provide twice the power and energy of a typical zinc-silver oxide battery. This battery type is based on silver oxide. Underwater applications like electrical control and guidance systems frequently use it. Because of its high theoretical specific energy and voltage, lightweight nature, high thermal and electrical conductivity, recyclability, affordable price, and capacity to produce three electrons per atom with high current density, aluminum is a great metal for use in batteries.

Al 1050 is the most popular and affordable option among aluminum alloys for an optimal anode in aluminum-silver oxide batteries. It provides a high negative OCP, an acceptable corrosion rate, high productivity and efficiency, safety as a battery anode, eco-friendliness, and affordability. Numerous aluminum batteries with alkaline electrolytes for a variety of applications have been developed as a result of the use of aluminum alloys [13].

Aluminum corrosion in batteries can cause several problems, including higher rates of spontaneous discharge, solid product-induced electrical resistance, deactivation of cathodic materials, and electrolyte contamination. As a result, maintaining aluminum corrosion control

is essential to the battery's longevity and effectiveness. Aluminum alloys have a passive protective layer (Al_2O_3) on their surface, which can pose challenges when used as a battery anode. In order to overcome this, electrolytes that dissolve this passive layer are frequently used to permit aluminum to corrode unhindered. Sodium hydroxide and potassium hydroxide are common solutions for removing this passive layer, but because aluminum corrodes quickly in these solutions, they are usually used in power-dense batteries [13]. Various methods have been employed to control the corrosion rate of aluminum anodes, with a particular focus on anode coating and alloying techniques. These methods have been extensively studied in alkaline environments and aluminum-air batteries. Examples include the application of nanocomposites as coatings on aluminum anodes [14], as well as the alloying of aluminum [15,16]. As it is known, alloying and surface coating approaches require a lot of production equipment, high costs and operator skills. To achieve a uniform corrosion of aluminum in neutral media, which is desirable for optimal battery performance, modifying the electrolyte by incorporating inhibitors, additives, or compound agents has proven to be a popular and effective approach. These additives can be categorized into organic and inorganic compounds, both of which are capable of controlling the self-corrosion of aluminum alloys [13]. However, it has been observed that each of the inhibitor compounds has major limitations, such that inorganic inhibitor compounds, due to their high price and the production of more toxic wastes and organic compounds, due to their lower stability in harsh corrosive conditions and high temperatures, it has led to limitations in the use and development of their applications. Therefore, in this research, the use of combined corrosion inhibitors, which use the advantages of each of the inorganic and organic compounds, has been adopted as a solution to overcome the aforementioned limitations and increase the productivity of electrolyte inhibitors.

Thiourea, an organosulfur compound containing oxygen, nitrogen, and sulfur atoms, serves as a corrosion inhibitor for aluminum alloy by adsorbing on the corroding surface and replacing water molecules with organic substances. This interaction in combination with common transition metal oxides inhibitors such ZnO helps prevent the transportation of corrosive ions to the surface, sustainably hindering cathodic or anodic corrosion reactions [13].

Therefore, the uniform corrosion characteristics of aluminum alloy 1050 were investigated in this study for the first time in an aerated 6.0 M KOH medium, both in the presence and absence of mixed ZnO/Thiourea inhibitor. The corrosion behavior was investigated using a variety of electrochemical tests, such as the polarization test and electrochemical impedance spectroscopy. In order to improve the performance of the Al/AgO battery, the localized corrosion behavior of aluminum in the environment was evaluated using scanning electron microscopy. Finally, the effectiveness of this additive in the battery was assessed using an AgO cathode and galvanostatic discharge test.

2. EXPERIMENTAL SECTION

2.1. Material and method

2.1.1. Preparation of materials and used solutions

Samples of Aluminum alloy 1050 with dimensions of 5×2 cm were prepared for polarization and impedance tests. Also, for weight loss measurements and microscopic examination, specimens were cut 2×2×2 from the selected aluminum sheet and subjected to grinding and degreasing steps.

2.2. Immersion test

Weight loss measurement was used to evaluate the potassium hydroxide solution at room temperature. The prepared samples were immersed for 5, 10, 15, 25, 40, and 60 minutes In 6 M potassium hydroxide solutions with adding the inhibitor in concentrations of 2, 4, 6, 8, and 10 g/L Thiourea and zinc oxide and washed and then carefully weighed after drying

.

2.3. Electrochemical tests

2.3.1. Determination of open circuit potential

The open-circuit potential of 1050 aluminum alloy immersed in 6.0 M potassium hydroxide solution containing different concentrations of thiourea and zinc oxide and their synergistic effect were investigated. In order to determine the open circuit potential, the Calomel electrode was used as the reference electrode. The data acquisition time was 60 minutes to determine the constant potential and reach a relatively steady state. The primary purpose of this test is to determine the time required for immersion before performing electrochemical tests such as polarization and impedance.

2.3.2. Linear polarization test

The potential to apply the corrosion rate of the working electrode was considered from negative 200 mV to positive 200 mV relative to the open circuit potential of the fragment in solution. The linear polarization test was conducted using a conventional three-electrode cell method using potentiostatic/galvanostatic Autolab PGSTAT 30, calomel electrode as a reference electrode, platinum electrode as an auxiliary electrode, and aluminum 1050 as the working electrode. Prior to performing all tests in the potassium hydroxide medium, the final tests, each sample was immersed in the solution for 10 minutes to achieve a stable relative state.

2.3.3. Electrochemical impedance test

The prepared aluminum samples were tested in 6 M potassium hydroxide solution with varying concentrations of the mentioned inhibitors after immersion for 10 minutes to achieve a stable equilibrium condition. The electrochemical impedance test was carried out using the

Schlumberger Frequency Response Device attached to the EG&G Model 237A Potentiostatic / Galvanostatic Device. Under open-circuit conditions, an alternating signal (AC) with a frequency range of 0.1 Hz to 100 kHz and an intensity of 10 mV was applied to perform the impedance test. Zsimpwin software was used to analyze the data obtained from both environments.

2.4. Sample Surface Analysis

Surface morphology was analyzed by an electron microscope equipped with X-ray diffraction spectroscopy after the absorbance of the inhibitors used in 6 M potassium hydroxide solution. For this purpose, aluminum 1050 was prepared. After preparation, the sample was immersed in potassium hydroxide for 1 hour in a solution, an optimal solution of thiourea, a solution containing the optimum amount of zinc oxide, and a solution containing the optimum amount of both were dipped and then analyzed. The device used for the study is TESCAN's MIRA3 MIRA3 (FE-SEM) Model Electron Microscope and has a resolution of 1.5 nm at a voltage of 15 kV, which provides an EDS detector.

2.5. Battery discharge test

To investigate the performance of thiourea and zinc oxide additives in the alkaline environment as a barrier to the aluminum anode in the battery and to evaluate the efficiency and performance of the battery, a galvanostatic discharge test was performed using silver oxide cathode in the environments mentioned above. The battery discharge test was performed in each of the mentioned environments for 30 minutes, and the test was performed in the absence of inhibitors and the optimum amount of simultaneous presence of zinc oxide and thiourea in an alkaline medium.

Also, in order to evaluate the efficiency of the aluminum anode as well as the battery capacity density, aluminum anodes were carefully weighed before and after discharge and calculated using the following equations: anode efficiency and capacity.

(1) $\eta(\%) = \frac{It}{\frac{\Delta mF}{9}}$

(2) $\text{Specific Capacity} = \frac{Ih}{\Delta m}$

Where *I* is the polarization current of the anode in A, *t* is the time in h, *Δm* is the weight loss in g, and *F* is the Faraday constant, and h is the time in hour.

3. RESULTS AND DISCUSSION

3.1. Immersion test

This test was used as a test to measure corrosion in order to accurately detect and observe changes in aluminum 1050 in potassium hydroxide.

The results in Tables S1 and 2 show that by adding different concentrations of thiourea inhibitors and zinc oxide to the solution, the corrosion rate of aluminum was significantly reduced.

Table 1. Polarization parameter of aluminum alloy 1050 in aerated 6.0 M potassium hydroxide solution in the presence of the thiourea / ZnO as a mixed inhibitor after 48 hours of immersion time, obtained from polarization plots

10g.lit $^{-1}$ conc of Thiourea+various concs of ZnO

Concentration of inhibitor	E (mV)	I_{corr} (A/cm^2)	β_a (V/dec)	$-\beta_c$ (V/dec)	R_p(Ω.cm^2)	C.R (mpy)	η
0	-1631	1.08×10^{-2}	0.177	0.133	3.10	4638.9	---
2	-1674	6.77×10^{-3}	0.198	0.133	5.10	2903.6	37.41
4	-1672	6.08×10^{-3}	0.165	0.129	5.18	2606.8	43.81
6	-1644	5.29×10^{-3}	0.171	0.113	5.58	2270.9	51.05
8	-1642	3.64×10^{-3}	0.131	0.123	7.58	1562.8	66.31
10	-1617	4.32×10^{-3}	0.136	0.125	6.55	1851.1	60.10

10g.lit $^{-1}$ conc of ZnO + various concs of Thiourea

Concentration of inhibitor	E (mV)	I_{corr} (A/cm^2)	β_a (V/dec)	$-\beta_c$ (V/dec)	R_p(Ω.cm^2)	C.R (mpy)	η
0	-1631	1.08×10^{-2}	0.177	0.133	3.10	4638.9	---
2	-1647	5.10×10^{-3}	0.176	0.139	6.60	2188.4	52.82
4	-1659	4.10×10^{-3}	0.154	0.133	7.57	1758.3	62.10
6	-1656	4.11×10^{-3}	0.158	0.141	7.86	1762.0	62.02
8	-1658	3.83×10^{-3}	0.158	0.138	8.34	1643.5	64.57
10	-1659	3.81×10^{-3}	0.158	0.138	8.36	1634.6	64.76

In order to analyze the data and complete the information gathered in the table above, the following steps were performed.

1. At first, after weighing the specimens using precision scales, the data obtained from weighting were extracted in Excel software and plotted in Figures 1 and 2. The diagonal slope of each diagram was then determined.
2. Using the formula below, the corrosion rate of each sample at different inhibitory concentrations was calculated.

$$(3)\ \text{Corrosion rate} = \frac{534.6 \times \Delta W}{D \times A \times t}$$

In which, ΔW represents the weight loss of the sample in mg, D represents the density of the sample in g.cm^{-3}, A represents the area of contact with the solution in inch^2, and t the immersion time in hr.

3. Next, the following formula was used to calculate the inhibition performance:

(4) $\eta\% = \frac{W_0 - W}{W_0} \times 100$

In which w_0 corrosion rate of aluminum sample in 6.0 M potassium hydroxide solution without inhibitor and W indicates the corrosion rate in the presence of a different concentration of inhibitors in the solution above [3].

According to the results, the addition of the inhibitor reduced the rate of corrosion by reducing the corrosion rate by 51% by forming a protective layer at 25 ° C.

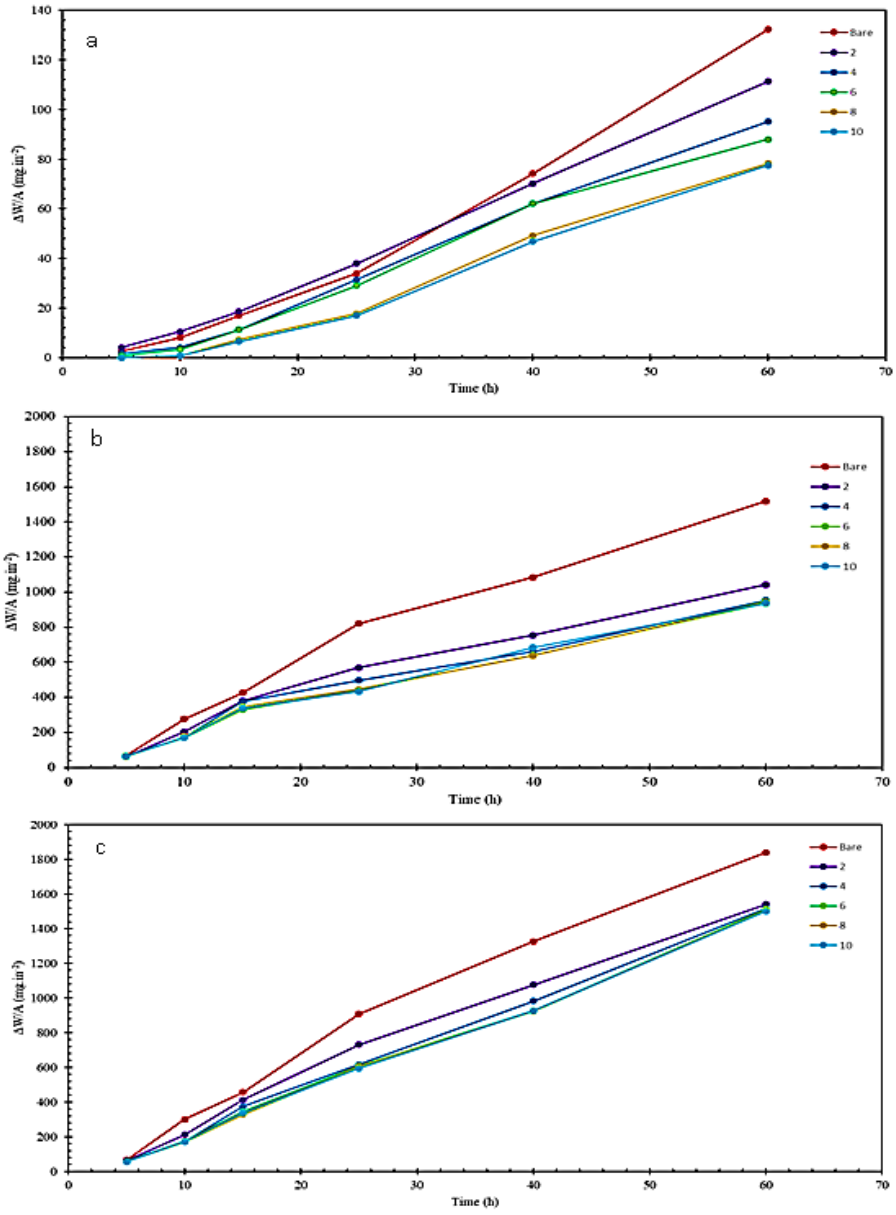

Figure 1. Graphs obtained from the immersion test of aluminum 1050 samples in 6.0 M potassium hydroxide environment in the presence of different concentrations of thiourea as a corrosion inhibitor at a) 5, b) 25, d) 65 °C for two weeks of immersion time

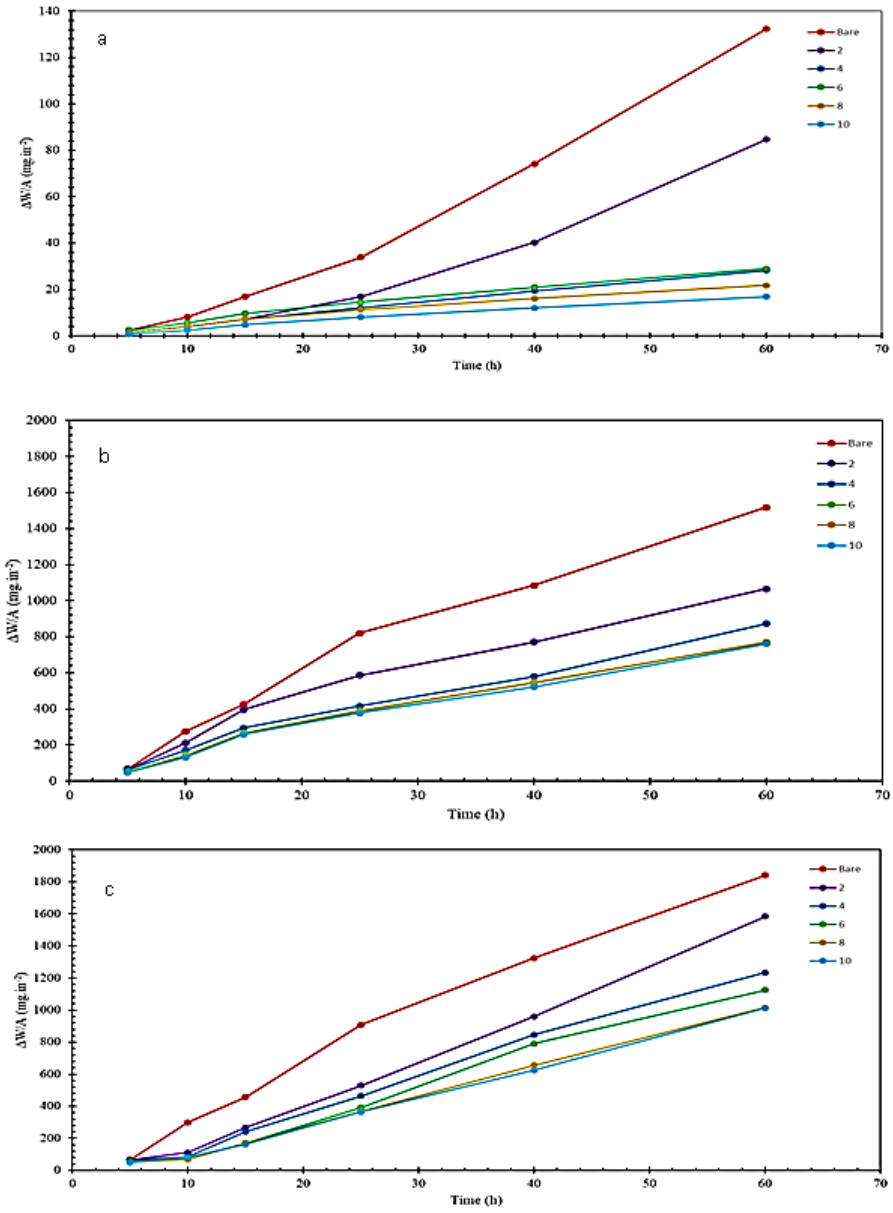

Figure 2. Graphs obtained from the immersion test of aluminum 1050 samples in 6.0 M potassium hydroxide environment in the presence of different concentrations of ZnO as a corrosion inhibitor at a) 5, b) 25, d) 65

3.2. Open circuit potential test

As shown in Figure 3, the diagrams corresponding to the open-circuit potential have a positive transition about the first 300 seconds and then reach a desirable steady state, thus providing an initial time to reach a steady state before conducting electrochemical tests such as polarization and impedance. They selected 10 minutes. It is further observed that the addition of the inhibitor, especially the thiourea inhibitor, had a transfer of about 100 mV to negative potentials indicating the effect of this inhibitor on the cathodic branch and disorder in this branch.

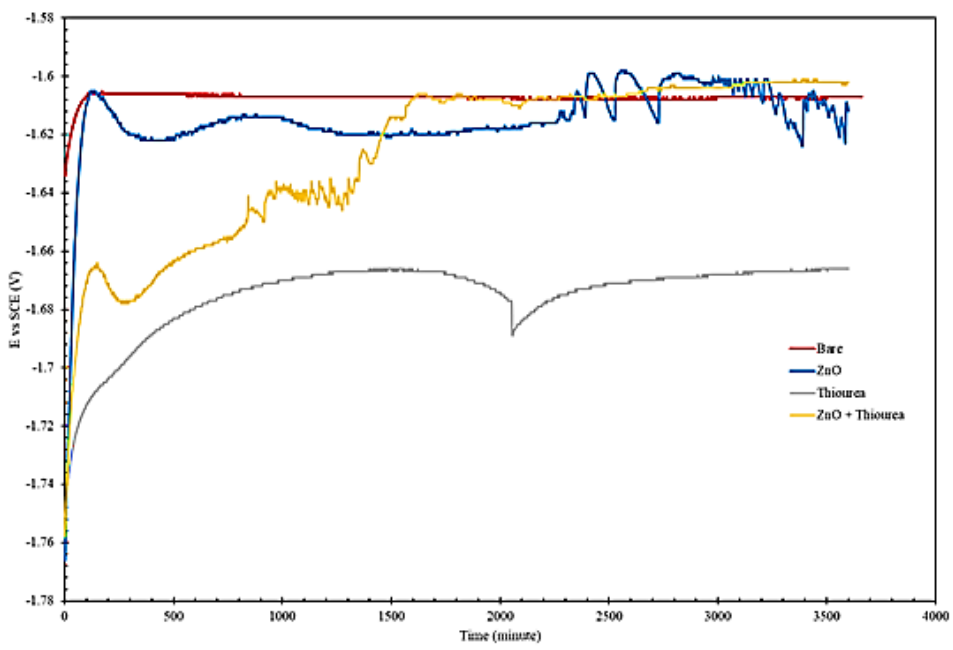

Figure 3. Open circuit potential changes during 60 minutes for aluminum alloy 1050 in the presence of thiourea and zinc oxide inhibitors and their simultaneous effect in 6.0 M potassium hydroxide Solution

3.3. Polarization test

This test was performed to investigate the accuracy of the results of the immersion test at ambient temperature on 1050 aluminum alloy. Initially, as shown in Figure S1, polarization curves of aluminum electrode in 6.0 M potassium hydroxide solution can be seen as an inhibitor in the presence and absence of zinc oxide. As expected, both the anodic and cathodic corrosion reactions of the aluminum electrode have been inhibited by increasing the amount of zinc oxide in the solution. In other words, the addition of ZnO reduced the anodic dissolution of aluminum and dramatically controlled the reaction rate of hydrogen gas release. As for the cause of such an event, it can be said that since Zn has a greater potential than aluminum to emit hydrogen gas, it results in the formation of a film on the aluminum metal surface which reduces the release of hydrogen gas onto the aluminum surface and thus corrodes Controls aluminum.

Table S3 shows data on polarization curves of aluminum alloys in potassium hydroxide solution in the absence and presence of different concentrations of zinc oxide. In this table, the corrosion potential, corrosion current density, anodic and cathodic slopes, polarization resistance, corrosion rate, and inhibition percentage are determined. According to this table, the density intensity of the Tafel curve is significantly reduced by adding zinc oxide to the electrolyte. The overall corrosion current intensity in the 1050 alloy is obtained by four-step interference, such that the dissolution of aluminum metal is partially dissolved and, after hydrogen gas release, a film of zinc oxide is formed on the surface and then, Zinc metal dissolution occurs with controlled aluminum dissolution. Thus, according to the results of the

graph and table, it can be seen that zinc oxide both reduces the rate of hydrogen release and delays the anodic branching and anodic dissolution of aluminum, indicating that this inhibition The actress acts as a mixed inhibitor. The important thing about the formation of this layer of zinc on the surface of aluminum is that it is easily separated from the surface and is generally a layer containing pores and pores that can be examined in the sample area by electron microscopy.

The inhibitory efficiency shown in Table S3 was obtained by using Equation, where i_0 is the corrosion current density without the addition of the inhibitor, and i is the value of the corrosion current density in the presence of the inhibitor in the above solution [17].

$$(5)\quad \eta\% = \frac{i_0 - i}{i_0} \times 100$$

Thiourea inhibitor is another substance that was added to the above solution by the polarization test. Figure S1 shows the Tafel graphs obtained from the polarization test of Aluminum 1050 samples in the presence of different concentrations of thiourea. Table S3 shows the data extracted from this graph for each case as a zinc oxide inhibitor. As can be seen in Figure S1, increasing the concentration of thiourea inhibitor in solution decreases the corrosion current density of 1050 alloy in 6.0 M potassium hydroxide. The reason for this decrease can be attributed to the uptake of molecules that block the active surfaces of the aluminum alloy. By absorbing these molecules on the surface, the sites are susceptible to corrosion, preventing them from being eaten and dissolved in the solution. According to the literature, if the diagram shows a corrosion potential greater than 90 mV, the inhibitor can be either anodized or cathodic, while in this test the maximum potential change during thiourea is about 50 It is a millivolt that indicates the complexity of this inhibitor as a zinc oxide inhibitor. Like zinc oxide, the addition of thiourea to the solution reduces the rate of release of hydrogen gas, which means that the inactivation by inactivating the active sites on the surface prevents the formation and formation of this gas and sulfur inside the thiourea structure. The toxins excrete hydrogen and protect the surface. Also, according to the polarization diagram and the current limit, one can find that the anodic reaction follows the influence. The addition of the inhibitor indicates that the inhibitor somehow controls the penetration and also prevents corrosion of the aluminum in this branch. According to the data obtained in the table, it is clear that adding 10 g/L of inhibitor up to 43% has a positive effect on the corrosion rate.

The effect of the combined use of both of the above inhibitors on the corrosion rate of aluminum was further investigated, and the idea arose that thiourea was used as an additive to smooth the copper onto the surface in addition to the electrodeposition properties of copper. Therefore, the addition of thiourea was expected not only to have a direct effect on the corrosion of aluminum due to the sulfur and nitrogen elements within its molecules but also to cause the uniformity of the layer of zinc oxide on the surface. Figure 4 shows the polarization

diagram of the polarization test in the presence of zinc oxide and thiourea at different concentrations.

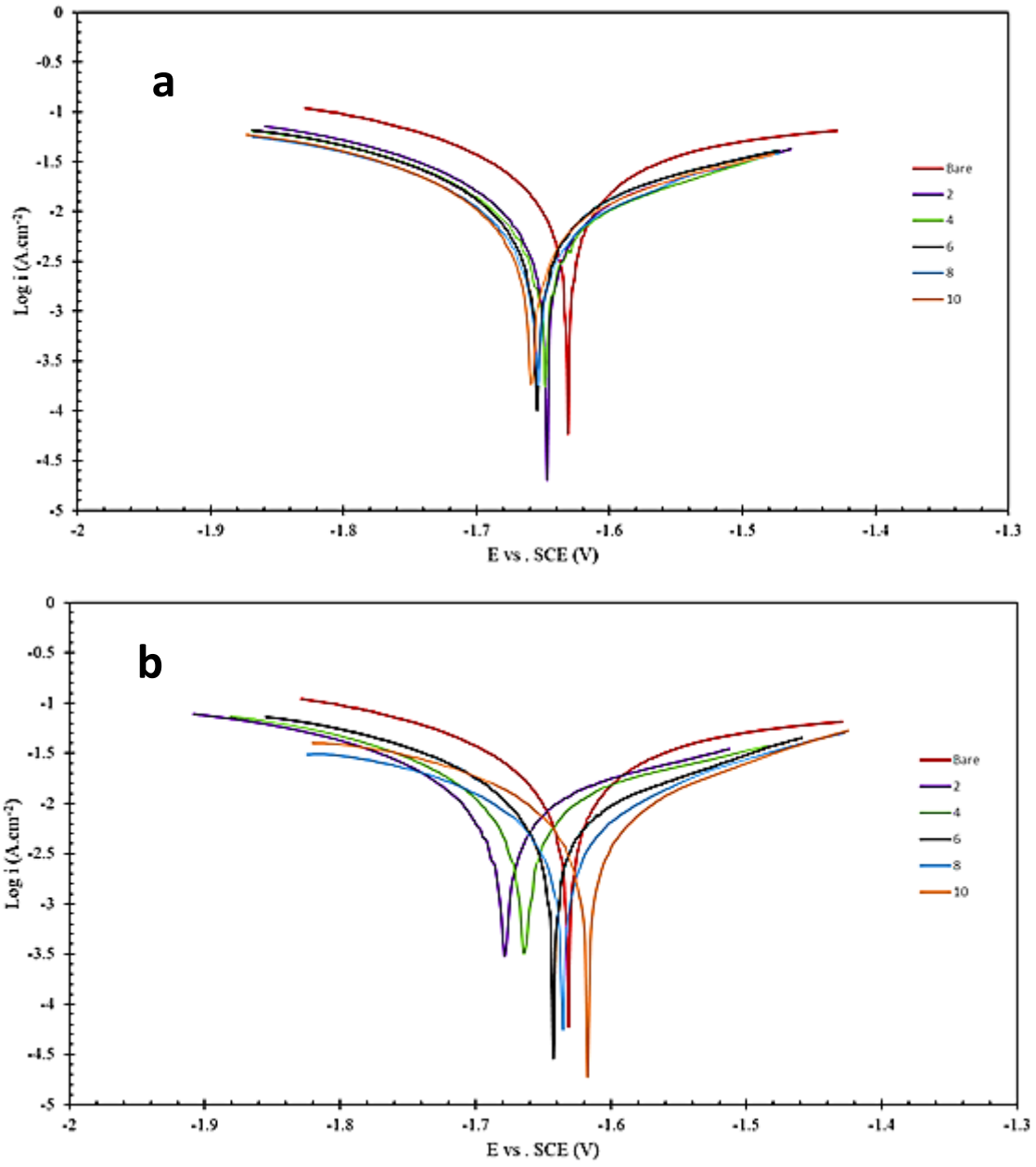

Figure 4. The Tafel plots obtained from the polarization test of aluminum alloy 1050 in the environment of 6.0 M potassium hydroxide in the presence of a) 10 g.lit^{-1} cons of thiourea and various concs of ZnO b) 10 g.lit^{-1} conc of ZnO and various concs of thiourea as a corrosion inhibitor

Table 1 also shows the results derived from the Tafel diagram for these inhibitors. In order to find the optimal concentration of each inhibitor at a constant concentration of each test, changes in the concentration of the inhibitor were considered. The results show that the addition of these two inhibitors together resulted in a significant improvement in the corrosion rate of

aluminum so during the test and afterward, it was found that the addition of thiourea prevents not only corrosion but also faster formation. The zinc oxide layer has a positive effect on the aluminum surface and creates a denser and more bonded layer on the surface, thus preventing the corrosion of aluminum in 6.0 M KOH solution as well.

3.4. Electrochemical impedance test

In order to study the effect of ZnO additive on the corrosion process of the electrode, the impedance of aluminum electrodes in 6.0 M potassium hydroxide solution was investigated in the presence of different concentrations of zinc oxide inhibitor in open-circuit potential, resulting from the curves in Figure S3 is shown. The presence of an inductive semicircle at high frequencies results from the ohmic drop, which has an imaginary part in the impedance and is related to the potential distribution on the electrode surface. The Nyquist curves of aluminum electrodes mainly consist of three parts: a capacitive semiconductor at high frequencies that results in electron transfer resistance in parallel with dual-layer capacitors, an inductive semiconductor at frequencies A medium resulting from the absorption of intermediate species and a capacitive semicircle at low frequencies resulting from the growth and dissolution of the surface film. The Nyquist diagrams using the circuits specified in Figure S3 are well fitted, and the results of these fittings are shown in Table S4. The presence of an inductor in the equivalent circuit indicates the formation of Al $(OH)_3$ film in the absence of ZnO and the formation of the Zn layer in the presence of the inhibitor.

As shown in the table, the solute resistance (R_s), load transfer resistance (R_{ct}), and dual-layer capacitor information are collected in this table. Since the capacitor does not follow the ideal behavior, a fuzzy time constant (CPE) containing an admixture (Y_0) and a power (n) is introduced to investigate the capacitor for a more accurate fit. And more suitable for equivalent circuits.

As shown in Table S4 and seen in the Nyquist diagram, the above three steps can be defined for zinc oxide inhibitors as the first ring formed at high frequencies related to zinc absorption and deposition. The surface is aluminum. The second semicircle involved the corrosion reaction and the conversion of aluminum to aluminum ion one times positive, which is expected to be the rate-controlling reaction of this reaction, so the resistance value of this ring represents the charge transfer resistance for The reaction is $Al \leftrightarrow Al^+$. Moreover, the last ring formed at low frequencies is corrosion and conversion of aluminum ion one positive to 3 times positive ion, which is done by $Al^+ \leftrightarrow Al^{3+}$. The efficiency of the inhibitors and the information about the dual-layer capacitors are obtained from the following relationships. Also, the polarization resistance reported in the table is determined from the relation [18].

$$(6)\ \eta\% = \frac{{R_{ct}}^{i} - R_{ct}}{R_{ct}} \times 100$$

$$(7)\ C_{dl} = Y_0(z\pi f_{max})^{n-1}$$

$$(8)\ R_p = \frac{R_{ct.1} \times R}{R_{ct.1} + R} + R_{ct.2}$$

The Niquistian curves of the aluminum electrodes show that as the concentration of zinc oxide increases, the charge transfer resistance increases, which can be attributed to the formation of zinc film on the aluminum surface. Increasing this charge transfer resistance indicates that the zinc oxide acts as a surface inhibitor and controls the electron transfer of the aluminum electrode corrosion process under open-circuit conditions.

Figure S2 shows the Nyquist diagram for aluminum 1050 in the presence of different concentrations of thiourea as a barrier in 6.0 M potassium hydroxide. As can be seen, the overall deformation of all the Nyquist diagrams of the aluminum electrodes is almost similar, indicating that the corrosion mechanism of aluminum does not change with increasing thiourea concentration and only increases corrosion resistance.

As can be seen, the Nyquist diagram of this alloy in the medium in the presence of different concentrations of thiourea contains three rings. The large capacitor loop created at high frequencies, the small inductive loop that was generated at medium frequencies, and the other capacitive loop that was located at low frequencies. The proposed equivalent circuit for this diagram is shown in Figure S2, which was used to calculate the relevant parameters collected in Table S4. The first semicircle at high frequencies can be attributed to the $Al \leftrightarrow Al^{+}$ reaction. This phase of charge transfer can be regarded as a step in controlling the overall corrosion rate. Therefore, the resistance value obtained from this step indicates the charge transfer resistance in the above reaction. The inductive ring formed at intermediate frequencies is due to the formation and absorption of intermediate phases on the aluminum surface upon dissolution of aluminum in the medium, and the last diagram ring is related to the $Al^{+} \leftrightarrow Al^{3+}$ conversion reaction.

As can be seen in the results shown in Table S1 and the diagrams and data fitting obtained by fitting in the presence of thiourea inhibitor, as the inhibitory concentration increases, the semicircular diameter increases indicating the adsorption of the molecule. The barrier is on the surface of the aluminum alloy. Increasingly, it is also seen that the load transfer resistance is also increased, which leads to a lower corrosion rate and improved corrosion behavior of aluminum.

According to the diagrams of Figures 5 and 6 related to the impedance of aluminum alloy in 6.0 M potassium hydroxide in the presence of two thiourea and zinc oxide inhibitors, mechanisms and rings formed for each step and their diameter only Increasingly, this indicates an increased corrosion resistance of the alloy in the environment. To justify the synchronous effect, it can also be said that the uniformity and stability of the zinc oxide coating improved upon the addition of thiourea and ultimately led to better corrosion control. The impedance results obtained from the addition of zinc oxide and thiourea, either alone or simultaneously,

as presented in Table 2 and Table S4, indicate and confirm the results of the polarization and immersion tests.

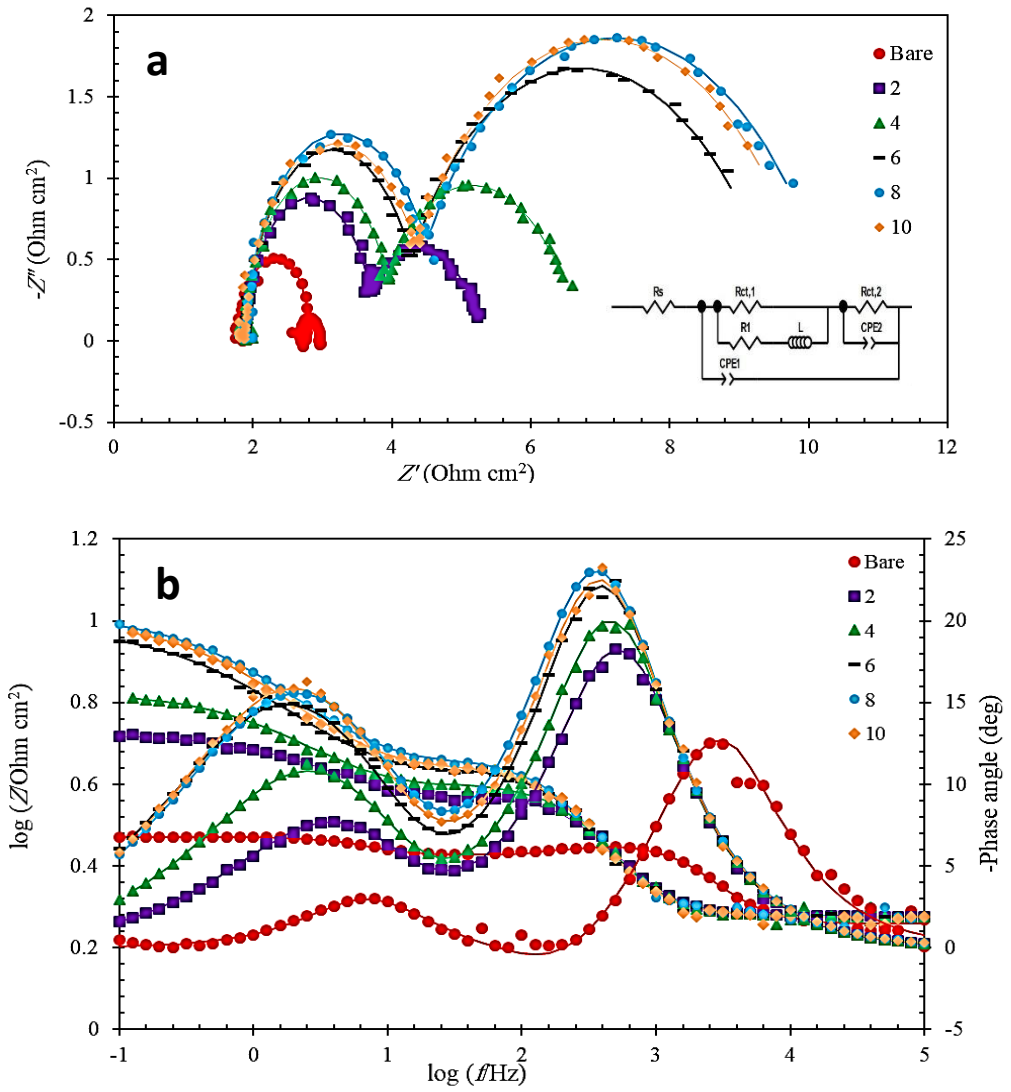

Figure 5. a) Nyquist and b) bode plots, resulting from the electrochemical impedance test of aluminum alloy 1050 in 6.0 M potassium hydroxide environment in the presence of 10 g.lit^{-1} conc of thiourea and various concs of ZnO as a corrosion inhibitor

3.5.Adsorption isotherms and thermodynamic parameters

In order to accurately investigate the interactions at the sample surface immersed in the solution, the adsorption isotherm is one of the most important measures to evaluate the performance of the inhibitors. The adsorption isotherm generally follows two general mechanisms, physical adsorption, and chemical adsorption. Due to the adsorption of the molecules on the aluminum surface, the corrosion rate decreases due to the overlapping of the active sites on the surface by the forming molecules. The percentage of surface coverage (θ)

shown in the table is equal to the inhibitory efficiency at different concentrations calculated from the three polarization and immersion and impedance tests.

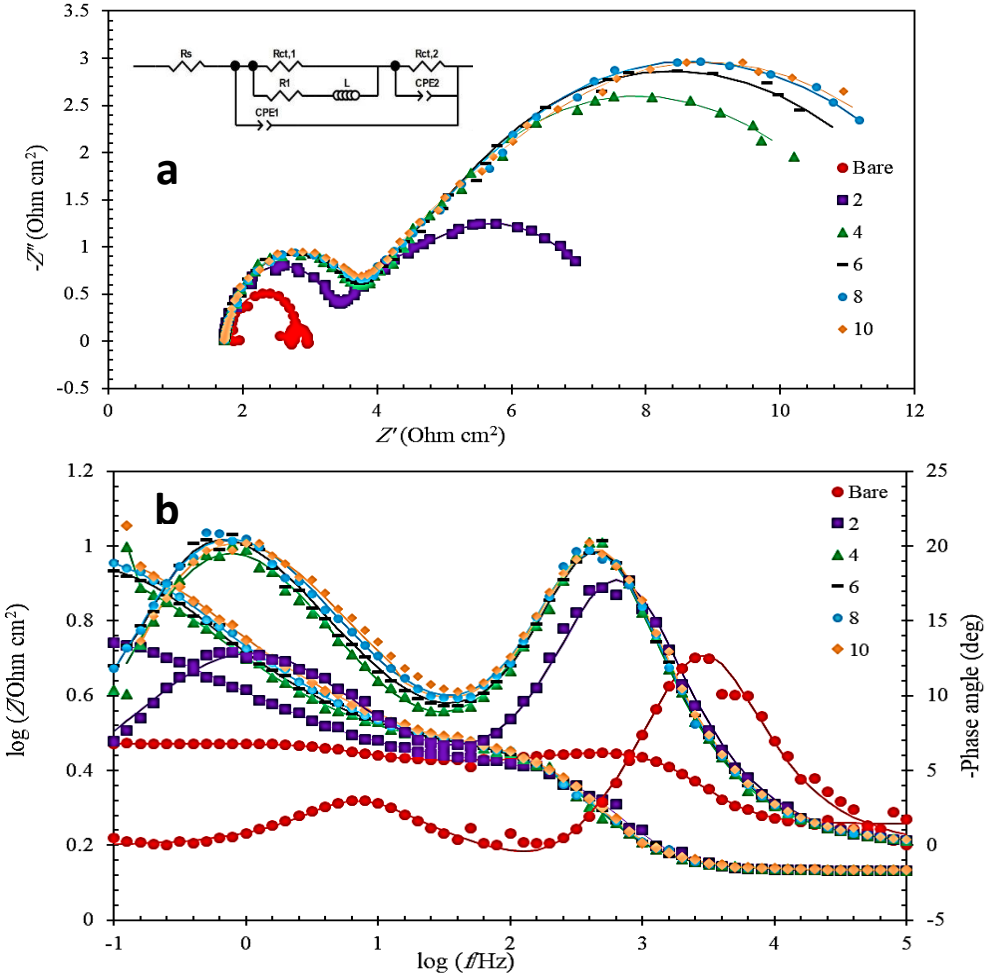

Figure 6. a) Nyquist and b) bode plots, resulting from the electrochemical impedance test of aluminum alloy 1050 in 6.0 M potassium hydroxide environment in the presence of 10 g.lit^{-1} conc of ZnO and various concs thiourea of as corrosion inhibitor

Table 2. EIS parameter during corrosion of aluminum alloy 1050 in aerated 6.0 M KOH solution in the presence of the Thiourea / ZnO as mixed inhibitor after 48 hours of immersion estimated by fitted with the proposed equivalent circuits

10g.lit $^{-1}$ conc of ZnO + various concs of Thiourea											
Concentration of inhibitor	R_s (Ω.cm^2)	CPE Y_0		R_{ct1} (Ω.cm^2)	L1	R1	CPE Y_0	n	R_{ct2} (Ω.cm^2)	R_p (Ω.cm2)	η
0	1.810	6.75×10^{-5}	023.1	1.023	0.004693	4.94	0.07818	1	0.30	1.15	---
2	1.720	3.01×10^{-4}	583.1	1.580	0.3493	0.79	0.06368	0.703	5.34	5.87	80.44
4	1.723	4.67×10^{-4}	831.1	1.831	0.3672	0.81	0.05132	0.685	9.47	10.03	88.56
6	1.724	4.71×10^{-4}	836.1	1.836	0.3721	0.88	0.05001	0.679	10.56	11.15	89.71
8	1.725	4.75×10^{-4}	840.1	1.840	0.3734	0.96	0.04673	0.674	11.10	11.73	90.22
10	1.727	4.80×10^{-4}	843.1	1.843	0.3776	1	0.04258	0.672	11.40	12.05	90.47

Adsorption isotherms include various models such as Temkin and Langmuir. Using the Excel software and the best linear fit in the diagrams of these models, the proposed adsorption isotherm for the inhibitor, Langmuir isotherm, is proposed using the following equation [3].

(9) $\frac{C}{\theta} = \frac{1}{K_{ads}} + C$

In which C represents the concentration of inhibitor used, K_{ads} represents the equilibrium constant of absorption, and θ the percentage of surface coverage. As shown in the figure, the Langmuir adsorption isotherm obtained from these three tests is plotted in which the R^2 value of all three graphs is very close to the unit, indicating the measurement accuracy for the isotherm modeling. The absorption equilibrium constant calculated in the above equation and the diagrams of Figure 7 is a useful parameter for determining the type of inhibitor on the surface. The aluminum fragment is such that by using the following equation, the free energy of absorption ΔG0ads can be calculated using this constant:

(10) $\Delta G^0{}_{ads} = -RTln(1000K_{ads})$

Where T is the test temperature in Kelvin, the global constant R of the gases, and 1000 times the concentration of water in the solution, the negativity of this value indicates the natural inhibition of the adsorption reaction on the sample surface. In general, if the energy is about -20 kJ / mol or more positive, the adsorption is only physical, and if it is at or below -40 kJ mol, the adsorption is purely chemical. The results in Table S5-8 show the physical absorption of selective inhibitors.

Also, in order to investigate the thermodynamic parameters of entropy and enthalpy, we examined the effect of temperature on the corrosion behavior of these two inhibitors separately, and it was observed that with decreasing corrosion rate, the adsorbent absorption was less spontaneous. Moreover, free energy is absorbed more positively. Also, with increasing temperature, the adsorption on the surface increases to near zero, but due to the high corrosion rate prevailing in the environment and due to the amount of surface covered by the inhibitor, the adsorption to the ambient temperature decreases.

3.6. Battery discharge test

As shown in Figure 8 and Table S11, the addition of the inhibitor has caused a slight decrease in the working potential of the aluminum anode in the aluminum oxide battery in the alkaline medium. By weighing the anode, before and after discharge, it was observed that the aluminum anode efficiency increased from 71.23% to 90.19%. Also, the battery capacity density in the non-inhibiting state was 2116.6 mAh / g, which increased the inhibitor to 2906.8 mAh / g, indicating that not only did the inhibitors above increase the efficiency and It does

not have a battery performance but rather reduced the corrosion rate of the aluminum anode, increasing the anode efficiency.

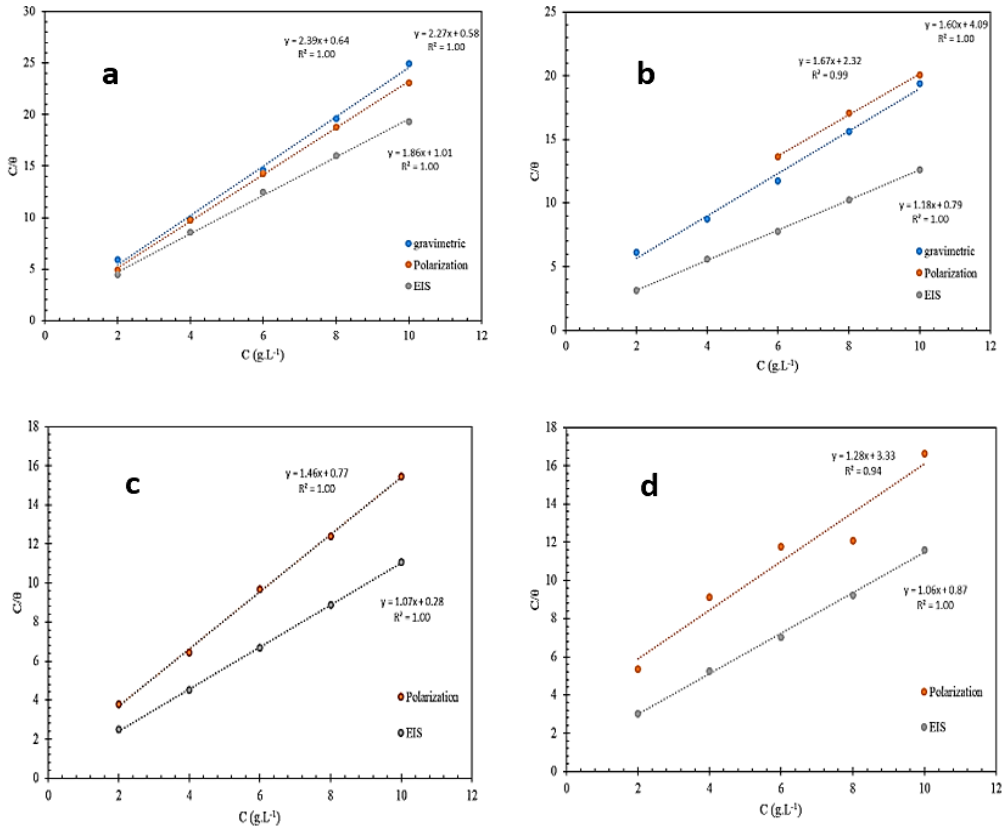

Figure 7. Langmuir isotherm diagrams obtained from immersion, polarization, and impedance tests in the presence of a) thiourea b) ZnO c) 10 g.lit^{-1} conc of ZnO and various concs thiourea d) 10 g.lit^{-1} conc of thiourea and various concs ZnO as corrosion inhibitors

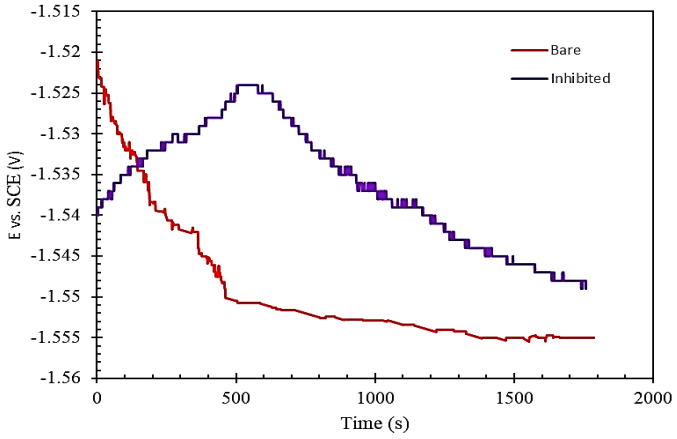

Figure 8. Galvanostatic discharge tests of the aluminum alloy 1050 as an Al/AgO battery anode in aerated 6.0 M KOH solution in the presence and absence of the ZnO/thiourea as an organic corrosion inhibitor

3.7. Sample Surface Analysis

The surface morphology of 1050 aluminum alloy fragments were obtained after 48-hour immersion in 6.0 M potassium hydroxide solution by electron microscopy. Figure 9 shows the level of aluminum in 1050 after being eaten without the presence of any additive as an inhibitor in said environment. The images show that the aluminum has folded and the formation of widespread cavities that have spread evenly over the surface.

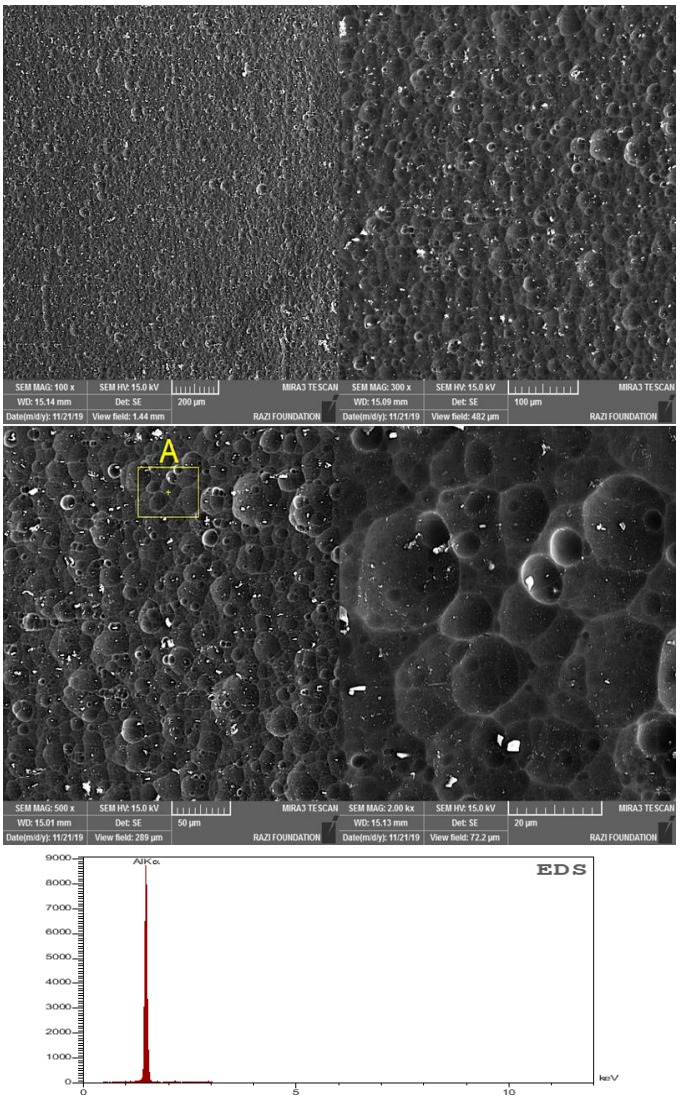

Figure 9. SEM images of the surface of the 1050 aluminum alloy sample after corrosion in 6.0 M potassium hydroxide environment for 48 hours in the absence of an inhibitor in the following magnifications: a) 100, b) 300, c) 500, d) 2000, and the obtained graph from the EDS spectrum

According to the results of Table S9, the post-roll surface contains only aluminum uniformly, and no additional peak is observed in EDS analysis. As can be seen in Figure S4, the addition of thiourea did not alter the surface morphology and only slightly reduced the radius of the formed cavities and attempted to smooth the corrosion surface. However,

according to Table S9, the addition of this inhibitor resulted in the formation of compounds containing carbon and oxygen on the surface, thus controlling the corrosion rate of aluminum in the environment.

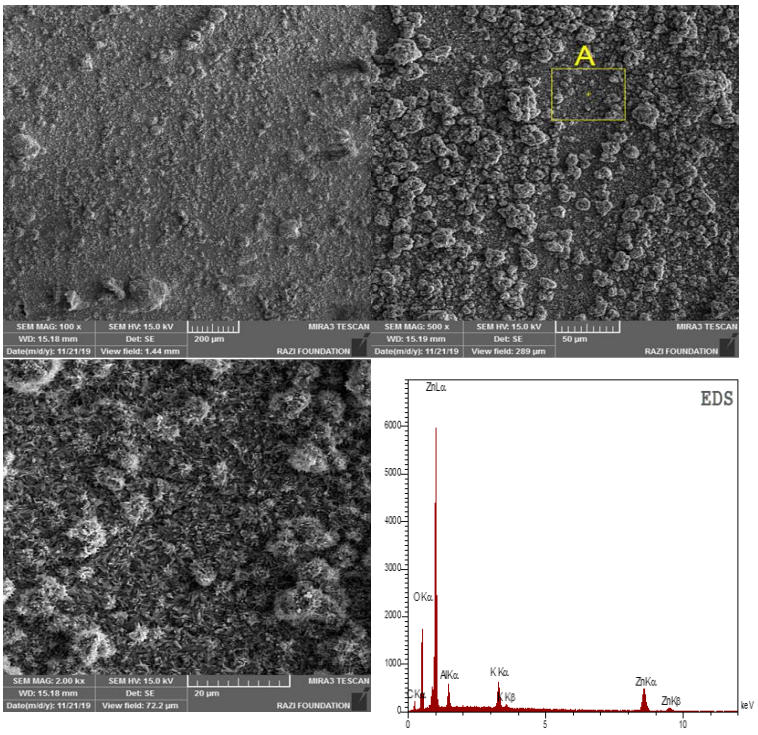

Figure 10. SEM images of the surface of the 1050 aluminum alloy sample after corrosion in 6.0 M potassium hydroxide environment for 48 hours in the presence of thiourea /ZnO inhibitor in the following magnifications: a) 100, b) 300, c) 500, d) 2000 and the obtained graph from the EDS spectrum

The addition of zinc oxide to the solution, as shown in Figure S5, by forming a thin layer of zinc precipitates, reduces the surface of the aluminum in contact with the solution and thereby fills the active corrosion sites on the surface, which results in a high aluminum corrosion rate control. The medium was potassium hydroxide. As can be seen in Table S9, the addition of zinc oxide by forming compounds containing zinc, oxygen, carbon, and potassium reduced the aluminum surface contact with the solution. As can be seen, this layer of coating, although well-bonded to the surface, is observed in some areas due to the lack of acceptable thickness of the layer. Also, the consistency of this layer is not acceptable. According to Figure 10, the simultaneous addition of zinc oxide and thiourea inhibitors resulted in the formation of a zinc-containing layer with better bonding and adhesion on the surface of the 1050 aluminum alloy, which confirms the increase in the amount of inhibition of this layer in the presence of thiourea ratio. It is time to be absent. According to Table S9, the amount of aluminum in contact with the solution, while both inhibitors were used concurrently, and the percentage of zinc present in the layer increased significantly, which meant that concurrent use led to the

formation of a continuous layer. And with very acceptable adhesion and thickness on the aluminum surface. According to the results of EDS, the presence of elemental zinc particles enables the formation of a porous film capable of producing controlled electrons, instead of being readily ingested by high-rate aluminum itself, which leads to the possible conduct of reactions. Below and provides the optimum corrosion rate control and anode.

(11) $ZnO + H_2O + 2OH^- \rightarrow Zn(OH)_4^{-2}$

(12) $3Zn(OH)_4^{-2} + 2Al \rightarrow 3Zn + 2Al(OH)_4^- + 4OH^-$

The XRD test was used to verify the accuracy of the EDS test results and to identify compounds formed on the aluminum surface when adding thiourea inhibitors and zinc oxide simultaneously, as shown in Figure S6 Using Xpert high score software, the peaks occurring in the graph were identified after identification, and the compounds corresponding to each peak identified and summarized in Table S10. According to this table, aluminum composites were identified as 18% metal substrate, 38% zinc, 18% zinc oxide, 19% thiourea, and 7% aluminum hydrogen sulfate composition on the aluminum surface. They indicated the accuracy of the EDS test results and the simultaneous presence of combinations of both inhibitors on the surface.

4. CONCLUSION

The following results are obtained from the corrosion tendencies of aluminum alloy 1050 in an aerated 6.0 M solution in the presence of thiourea as an inhibitor:

a) According to the EIS and polarization analyses, the inhibitor reduced the aluminum's corrosion rate by forming a shielding film on the surface during the early phase. This film controls the anode's self-corrosion and the aluminum's oxide layer's potential to passivate the surface, which ultimately results in a decrease in battery efficiency.

b) The Al/AgO battery's aluminum anode can corrode in a controlled way and at a specific rate with the introduction of an inhibitor. The EIS, polarization, and galvanostatic discharge tests all show that this improves the battery's performance and increases the aluminum anode's efficiency.

c) The SEM observations reveal that the presence of thiourea as a corrosion inhibitor significantly decreases the likelihood of both pit initiation and propagation on the aluminum anode's surface. This creates conditions for uniform corrosion of the anode, resulting in enhanced battery performance.

Acknowledgments

The University of Tehran is greatly appreciated by the authors for providing the facilities needed to complete this major research project.

Declarations of interest

The authors declare that none of the work reported in this article could be influenced by known competing financial interests or personal relationships.

REFERENCES

[1] H. Pourfarzad, M. Shabani-Nooshabadi, and M.R. Ganjali, J. Power Sources 451 (2020) 1.
[2] H. Pourfarzad, M. Shabani-Nooshabadi, and M.R. Ganjali, Electrochim. Acta 317 (2019) 83.
[3] H. Pourfarzad, M. Shabani-Nooshabadi, and M.R. Ganjali, J. Mol. Liq. 302 (2020) 1.
[4] H. Pourfarzad, M. Shabani-Nooshabadi, and M.R. Ganjali, Composites Part B: Engineering 193 (2020) 1.
[5] H. Pourfarzad, R. Badrnezhad, M. Ghaemmaghami, and M. Saremi, Ionics 27 (2021) 4057.
[6] H. Pourfarzad, M. Saremi, R. Badrnezhad, J. Mater. Sci.: Mater. Electron. 32 (2021) 17602.
[7] R. Badrnezhad, F. Nasri, H. Pourfarzad, and S.K. Jafari, Int. J. Hydrogen Energy 46 (2021) 3821.
[8] A.N. Sadr, F. Nasri, H. Pourfarzad, N. Manavizadeh, M.Z. Pedram, and G.A. Naikoo, Adv. Mater. Technol. (2022) 2100986.
[9] H. Pourfarzad, M. Saremi, S. Khadem Jafari, R. Jazmi, and R. Badrnezhad, Anal. Bioanal. Electrochem. 14 (2022) 486.
[10] H. Pourfarzad, M. Karimi, M. Saremi, and R. Badrnezhad, Anal. Bioanal. Electrochem. 14 (2022) 696.
[11] R. Badrnezhad, and A. Fathollahi Zonouz, Anal. Bioanal. Electrochem. 14 (2022) 160.
[12] H. Pourfarzad, M.H. Olia, A. Shirojan, M.R. Ganjali, and R. Rahighi, Russian J. Electrochem. 54 (2018) 1053.
[13] M. Peirow Asfia, H. Pourfarzad, H. Kashani, M.H. Olia, and R. Badrnezhad, J. Electrochem. Soc. 167 (2020) 140527.
[14] X. Huang, H. Mutlu, and P. Théato, Colloid Polym. Sci. 299 (2021) 325.
[15] C. Wang, T. Chen, Y. Liu and et al, ACS Energy Lett. 8 (2023) 2252.
[16] M. Song, and Z. Zhang, Nano Res. 17 (2024) 1366.
[17] A.R. Madram, H. Pourfarzad, and H.R. Zare, Electrochim. Acta 85 (2012) 263.
[18] R. Badrnezhad, H. Pourfarzad, A.R. Madram, and M.R. Ganjali, Russian J. Electrochem. 55 (2019) 272.